Elementary excitations in an integrable twisted $J_1 - J_2$ spin chain in the thermodynamic limit

Wei Wang[1,2] Yi Qiao,[2] Rong-Hua Liu,[1] Wu-Ming Liu[2,3,4,*] and Junpeng Cao[2,3,4,5,†]

[1]*National Laboratory of Solid State Microstructures, School of Physics and Collaborative Innovation Center of Advanced Microstructures, Nanjing University, Nanjing 210093, China*
[2]*Beijing National Laboratory for Condensed Matter Physics, Institute of Physics, Chinese Academy of Sciences, Beijing 100190, China*
[3]*School of Physical Sciences, University of Chinese Academy of Sciences, Beijing 100049, China*
[4]*Songshan Lake Materials Laboratory, Dongguan, Guangdong 523808, China*
[5]*Peng Huanwu Center for Fundamental Theory, Xian 710127, China*

The exact elementary excitations in a typical $U(1)$ symmetry broken quantum integrable system, that is the twisted $J_1 - J_2$ spin chain with nearest-neighbor, next nearest neighbor, and chiral three spin interactions, are studied. The main technique is that we quantify the energy spectrum of the system by the zero roots of the transfer matrix instead of the traditional Bethe roots. From the numerical calculation and singularity analysis, we obtain the patterns of zero roots. Based on them, we analytically obtain the ground state energy and the elementary excitations in the thermodynamic limit. We find that the system also exhibits the nearly degenerate states in the regime of $\eta \in \mathbb{R}$, where the nearest-neighbor couplings among the z direction are ferromagnetic. More careful study shows that the competing of interactions can induce the gapless low-lying excitations and quantum phase transition in the antiferromagnetic regime with $\eta \in \mathbb{R} + i\pi$.

I. INTRODUCTION

Understanding the collective behavior in the one-dimensional quantum many-body systems is a fascinating and challenging issue. Due to the competition of some kinds of interactions, many novel physical phenomena are found, and new physical pictures are developed. The exact solution can provide the benchmark of these new theories [1–3]. The typical methods of seeking the exact solution are the coordinate [4] and algebraic Bethe ansatz [5–11], as well as the $T - Q$ relation [12,13]. These methods are powerful when studying quantum integrable systems with $U(1)$ symmetry. However, if the $U(1)$ symmetry is broken, it is hard to construct a suitable reference state and to apply these methods. On the other hand, based on the Yang-Baxter equation and reflection equations, we can prove that there indeed exist some quantum integrable systems without $U(1)$ symmetry. The next problem is how to solve them exactly. Then many interesting methods such as gauge transformation [14], $T - Q$ relation based on the fusion [15,16], q-Onsager algebra [17,18], separation of variables [19,20], modified algebraic Bethe ansatz [21–23], and off diagonal

Bethe ansatz [24,25] have been developed. We should note that the exact solutions of quantum integrable systems without $U(1)$ symmetry have many applications in non-equilibrium statistical mechanics [26,27], topological physics [28,29], and high energy physics [30–34].

The next question is how to calculate the exact physical quantities of the systems in the thermodynamic limit. The difficulties come from the eigenvalues, and the associated Bethe ansatz equations (BAEs) are inhomogeneous. Thus, it is impossible to take the logarithm of BAEs and use the thermodynamic Bethe ansatz. Recently, a novel Bethe ansatz scheme has been proposed to calculate the physical quantities of quantum integrable systems with or without $U(1)$ symmetry to overcome the obstacles [35,36]. The main idea is that the eigenvalues of the transfer matrix can be characterized by their zero roots instead of the traditional Bethe roots.

In this paper, we study an integrable $J_1 - J_2$ spin chain, which includes the nearest-neighbor (NN), next-nearest-neighbor (NNN), and chiral three-spin interactions. The boundary condition is the antiperiodic one. The twisted boundaries break the $U(1)$ symmetry of the system. After the boundary reflection, the spins of quasiparticles are not conserved. Based on the algebraic analysis, we obtain the energy spectrum of the system and the homogeneous BAEs. From the numerical calculation and singularity analysis of BAEs, we get the distributions of solutions

*Corresponding author.
wmliu@iphy.ac.cn

†Corresponding author.
junpengcao@iphy.ac.cn

056005-1

in the thermodynamic limit. Then, we compute the ground state energy and elementary excitations. We also find the nearly degenerate states in the ferromagnetic regime and the quantum phase transition in the antiferromagnetic regime.

The paper is organized as follows. The next section serves as an introduction to the antiperiodic $J_1 - J_2$ spin chain and the explanation of its integrability. In Sec. III, we give the eigenvalues spectrum. In Sec. IV, combined with the inhomogeneous $T - Q$ relation, we analyse the zero root patterns of the eigenvalue of the transfer matrix. We study the nearly degenerate states in Sec. V. Then, we calculate the ground state energy and low-lying excitations in the thermodynamic limit focusing on the regime of real in Sec. VI. In Sec. VII, the exact physical properties are discussed in the regime of $\eta \in \mathbb{R} + i\pi$. Concluding remarks and discussions are given in Sec. VIII.

II. THE SYSTEM AND INTEGRABILITY

The Hamiltonian of the integrable anisotropic $J_1 - J_2$ model reads

$$
H = -\sum_{j=1}^{2N} \sum_{\alpha=x,y,z} [J_1^\alpha \sigma_j^\alpha \sigma_{j+1}^\alpha + J_2 \sigma_j^\alpha \sigma_{j+2}^\alpha
$$
$$
+ (-1)^j J_3^\alpha \sigma_{j+1}^\alpha (\vec{\sigma}_j \times \vec{\sigma}_{j+2})^\alpha], \qquad (2.1)
$$

as shown in Fig. 1. Here, $2N$ is the number of sites. $\{\sigma_j^\alpha | j = 1, \ldots, 2N\}$ are the 2×2 Pauli matrices along the α direction at the jth site. In this paper, we consider the system (2.1) with antiperiodic boundary condition,

$$
\sigma_{2N+n}^\alpha = \sigma_n^x \sigma_n^\alpha \sigma_n^x, \quad n = 1, 2, \qquad \alpha = x, y, z, \qquad (2.2)
$$

which gives $\sigma_{2N+n}^x = \sigma_n^x$, $\sigma_{2N+n}^y = -\sigma_n^y$, and $\sigma_{2N+n}^z = -\sigma_n^z$. J_1^α quantifies the NN coupling with the form of

$$
J_1^x = J_1^y = \cosh(2a), \qquad J_1^z = \cosh\eta, \qquad (2.3)
$$

where a is the model parameter and η is the anisotropic parameter. J_2 characterizes the NNN isotropic coupling,

$$
J_2 = -\frac{\sinh^2(2a)\cosh\eta}{2\sinh^2\eta}. \qquad (2.4)
$$

J_3^α describes the chiral three-spin coupling with the strength of

$$
J_3^x = J_3^y = \frac{i\sinh(2a)}{2\sinh\eta}\cosh\eta, \qquad J_3^z = \frac{i\sinh(4a)}{4\sinh\eta}. \qquad (2.5)
$$

If $a = 0$, the model (2.1) degenerates into the Heisenberg spin chain. It is worth mentioning that the Hermitian operator of Hamiltonian (2.1) requires that a must be real
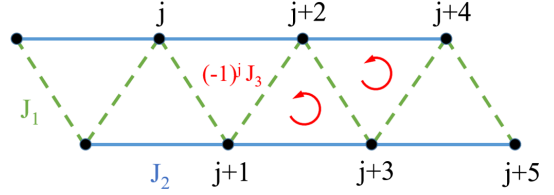

FIG. 1. Illustration of the bulk of twisted $J_1 - J_2$ spin system with the nearest-neighbor interactions J_1, next-nearest-neighbor interactions J_2, and chiral three-spin interactions $(-1)^j J_3$. The model can be viewed as the zigzag chain. The order of the chiral three-spin coupling in each triangle is indicated by the red arrows.

if η is imaginary, and a must be imaginary if η is real or $\eta \in \mathbb{R} + i\pi$.

Now, we show that the model (2.1) is integrable, which is related to the six-vertex R matrix,

$$
R_{0,j}(u) = \frac{\sinh(u+\eta) + \sinh u}{2\sinh\eta} + \frac{1}{2}(\sigma_j^x \sigma_0^x + \sigma_j^y \sigma_0^y)
$$
$$
+ \frac{\sinh(u+\eta) - \sinh u}{2\sinh\eta}\sigma_j^z \sigma_0^z, \qquad (2.6)
$$

where u is the spectral parameter. Throughout this paper, we adopt the standard notations. For any matrix $A \in \text{End}(\mathbb{C})$, A_j is an embedding operator in the tensor space $\mathbb{C}^2 \otimes \mathbb{C}^2 \otimes \cdots$, which acts as A on the jth space and as an identity on the other factor spaces. $R_{0,j}(u)$ is an embedding operator of R matrix in the tensor space, which acts as identity on the factor spaces except for the 0th and jth ones. Here 0 means the auxiliary space and $j = 1, \ldots, 2N$ means the physical or quantum space. The R matrix (2.6) has the following properties:

$$
\text{Initial condition:} \quad R_{0,j}(0) = P_{0,j}, \qquad (2.7)
$$

$$
\text{Unitarity relation:} \quad R_{0,j}(u)R_{j,0}(-u) = \phi(u) \times \mathbf{id}, \qquad (2.8)
$$

$$
\text{Crossing relation:} \quad R_{0,j}(u) = V_0 R_{0,j}^{t_j}(-u-\eta)V_0,
$$
$$
V_0 = -i\sigma_0^y, \qquad (2.9)
$$

$$
\text{PT symmetry:} \quad R_{0,j}(u) = R_{j,0}(u) = R_{0,j}^{t_0 t_j}(u), \qquad (2.10)
$$

$$
Z_2 \text{ symmetry:} \quad \sigma_0^\alpha \sigma_j^\alpha R_{0,j}(u) = R_{0,j}(u)\sigma_0^\alpha \sigma_j^\alpha,
$$
$$
\text{for } \alpha = x, y, z, \qquad (2.11)
$$

$$
\text{Quasiperiodicity:} \quad R_{0,j}(u+i\pi) = -\sigma_0^z R_{0,j}(u)\sigma_0^z, \qquad (2.12)
$$

$$
\text{Fusion relation:} \quad R_{0,j}(-\eta) = -2P_{0,j}^{(-)}. \qquad (2.13)
$$

Here, $\phi(u) = -\sinh(u+\eta)\sinh(u-\eta)/\sinh^2\eta$, **id** is the identity operator, $R_{j,0}(u) = P_{0,j}R_{0,j}(u)P_{0,j}$ with $P_{0,j}$ being the permutation operator, t_l denotes transposition in the lth

space, and $P_{0,j}^{(-)}$ is the one-dimensional antisymmetric projection operator, $P_{0,j}^{(-)} = (1 - P_{0,j})/2$. Besides, the R matrix (2.6) satisfies the Yang-Baxter equation,

$$R_{0,j}(u_1 - u_2)R_{0,l}(u_1 - u_3)R_{j,l}(u_2 - u_3)$$
$$= R_{j,l}(u_2 - u_3)R_{0,l}(u_1 - u_3)R_{0,j}(u_1 - u_2). \quad (2.14)$$

We combine all the R matrices in different sites and define the monodromy matrix as

$$T_0(u) = \sigma_0^x R_{0,1}(u - \theta_1)R_{0,2}(u - \theta_2)$$
$$\cdots R_{0,2N-1}(u - \theta_{2N-1})R_{0,2N}(u - \theta_{2N}), \quad (2.15)$$

where the $\{\theta_j | j = 1, \ldots, 2N\}$ are the inhomogeneous parameters. The transfer matrix is given by tracing the monodromy matrix in the auxiliary space,

$$t(u) = \text{tr}_0 T_0(u). \quad (2.16)$$

Based on the commutation relation (2.11) and the Yang-Baxter equation (2.14), one can prove that the transfer matrices with different spectral parameters commute with each other, i.e.,

$$[t(u), t(v)] = 0. \quad (2.17)$$

Expanding the transfer matrix with respect to the spectral parameter u, all the expansion coefficients are also commutative. According to the quantum integrable theory, all the conserved quantities including the model Hamiltonian can be constructed by these expansion coefficients. Because the number of independent conserved quantities equals to that of the degrees of freedom, the system is integrable.

The Hamiltonian (2.1) is generated by the transfer matrices as

$$H = \phi^{1-N}(2a)\sinh\eta \left\{ t(a - \eta)\frac{\partial t(u)}{\partial u}\Big|_{u=a} \right.$$
$$\left. + t(-a - \eta)\frac{\partial t(u)}{\partial u}\Big|_{u=-a} \right\}\Big|_{\{\theta_j = (-1)^j a\}} + E_0, \quad (2.18)$$

where the constant E_0 is given by

$$E_0 = -\frac{N\cosh\eta[\cosh^2(2a) - \cosh(2\eta)]}{\sinh^2\eta}. \quad (2.19)$$

Another interesting conserved quantity is the shift operator, which is generated by the transfer matrix as [37]

$$U = \phi^{-N}(2a)t(a)t(-a)|_{\{\theta_j = (-1)^j a\}}. \quad (2.20)$$

One can find that the operator U commutate with the Hamiltonian. The U characterizes the transition invariance

of the present system. According to the quantum theory, we can define the topological momentum k as

$$k = -i\ln U = -i\sum_{j=1}^{2N-1}\ln\frac{\sinh(a + z_j - \frac{\eta}{2})}{\sinh(a - z_j - \frac{\eta}{2})}\text{mod}\{2\pi\}. \quad (2.21)$$

III. THE EIGENVALUES SPECTRUM

From the construction (2.18), we know that the eigenenergies of the Hamiltonian (2.1) are related with the eigenvalues of transfer matrix $t(u)$. If the eigenvalues of the transfer matrix are known, the eigenenergies are known. Thus, we diagonalize the transfer matrix $t(u)$ first. Because the $U(1)$ symmetry of the system is broken, we calculate the eigenvalues of transfer matrix based on the polynomial analysis. The main ideas are as follows. From the definitions (2.6), (2.15), and (2.16), we know that the transfer matrix $t(u)$ is an operator-valued trigonometric polynomial with degree $2N - 1$ due to the existence of twisted matrix σ_0^x and partial trace. According to the algebra analysis theory, the values of $t(u)$ can be completely determined by the $2N - 1$ independent constraints. Then, we should seek these constraints, which can be achieved by using the fusion technique. At the inhomogeneous point θ_j, the R matrix (2.6) degenerates into the one-dimensional projector operator; please see Eq. (2.13). By using the properties of projector and Yang-Baxter equation, we can obtain the transfer matrices product identities in these one-dimensional subspaces characterized by $\{\theta_j | j = 1, \ldots, 2N\}$. At the certain values of spectral parameter, these identities are closed and can be used to determine the eigenvalues of $t(u)$. The more detailed description can be found in Ref. [24] or Chap. 4 in the book [25].

By using the initial condition (2.7), we have

$$t(\theta_j) = \text{tr}_0\{\sigma_0^x R_{0,1}(\theta_j - \theta_1)\cdots P_{0,j}$$
$$\cdots R_{0,2N-1}(\theta_j - \theta_{2N-1})R_{0,2N}(\theta_j - \theta_{2N})\}$$
$$= R_{j,j+1}(\theta_j - \theta_{j+1})\cdots R_{j,2N}(\theta_j - \theta_{2N})\sigma_j^x R_{j,1}(\theta_j - \theta_1)$$
$$\cdots R_{j,j-1}(\theta_j - \theta_{j-1}); \quad (3.1)$$

with the help of crossing relation (2.9), the transfer matrix $t(\theta_j - \eta)$ can be calculated as

$$t(\theta_j - \eta) = (-1)^{2N-1}R_{j,j-1}(-\theta_j + \theta_{j-1})\cdots R_{j,1}(-\theta_j + \theta_1)$$
$$\times \sigma_j^x R_{j,2N}(-\theta_j + \theta_{2N})\cdots R_{j,j+1}(-\theta_j + \theta_{j+1}). \quad (3.2)$$

Multiplying Eqs. (3.1) and (3.2), and using the unitarity relation (2.8), we obtain the following operators product identities:

TABLE I. The zero roots and energy spectrum of the system (2.1) with $2N = 4$, $a = 0.2i$, and $\eta = 0.8$. Here, E_n is the eigenenergy of the nth level, and each level is double degenerate.

z_1	z_2	z_3	E_n	n
$-0.4614i$	0	$0.4614i$	-4.3679	1
$-0.3430i$	$0.0949i$	$0.9096i$	-3.4531	2
$-0.9096i$	$-0.0949i$	$0.3430i$	-3.4531	3
$-1.5708i$	$-0.2291i$	$0.2291i$	-3.2656	4
$-1.0545 - 1.5708i$	0	$1.0545 - 1.5708i$	0.6836	5
$-0.8175 + 0.2545i$	$-0.2764i$	$0.8175 + 0.2545i$	3.4531	6
$-0.8175 - 0.2545i$	$+0.2764i$	$0.8175 - 0.2545i$	3.4531	7
-0.8212	$-1.5708i$	0.8212	6.9499	8

$$t(\theta_j)t(\theta_j - \eta) = -a(\theta_j)d(\theta_j - \eta) \times \mathbf{id}, \quad j = 1, \ldots, 2N, \tag{3.3}$$

where

$$d(u) = a(u - \eta) = \prod_{j=1}^{2N} \frac{\sinh(u - \theta_j)}{\sinh \eta}. \tag{3.4}$$

Denote the eigenvalue of $t(u)$ as $\Lambda(u)$. Acting the operator identities (3.3) on a common state of $t(u)$ and $t(u - \eta)$, we obtain the following functional relations:

$$\Lambda(\theta_j)\Lambda(\theta_j - \eta) = -a(\theta_j)d(\theta_j - \eta), \quad j = 1, \ldots, 2N. \tag{3.5}$$

The eigenvalue $\Lambda(u)$ is a trigonometric polynomial of u with the degree $2N - 1$. Thus, the value of $\Lambda(u)$ can be completely determined by the $2N$ constraints (3.5).

Besides, the transfer matrix $t(u)$ satisfies the periodicity,

$$t(u + i\pi) = (-1)^{2N-1}t(u), \tag{3.6}$$

which gives

$$\Lambda(u + i\pi) = (-1)^{2N-1}\Lambda(u). \tag{3.7}$$

According to Eqs. (3.5) and (3.7), we express $\Lambda(u)$ in terms of its $2N - 1$ zero roots $\{z_j - \eta/2 | j = 1, \ldots, 2N - 1\}$ and an overall coefficient Λ_0 as

$$\Lambda(u) = \Lambda_0 \prod_{j=1}^{2N-1} \sinh\left(u - z_j + \frac{\eta}{2}\right). \tag{3.8}$$

Substituting the parametrization (3.8) into (3.5), we obtain the constraints among zero roots,

$$\Lambda_0^2 \prod_{j=1}^{2N-1} \sinh\left(\theta_l - z_j + \frac{\eta}{2}\right) \sinh\left(\theta_l - z_j - \frac{\eta}{2}\right) = -\sinh^{-4N}\eta \prod_{j=1}^{2N} \sinh(\theta_l - \theta_j + \eta) \times \sinh(\theta_l - \theta_j - \eta), \quad l = 1, \ldots, 2N. \tag{3.9}$$

We note the BAEs (3.9) are homogeneous. From the construction (2.18), we obtain the energy spectrum of Hamiltonian (2.1) as

$$E = \phi^{1-N}(2a) \sinh \eta \left\{ \Lambda(a - \eta) \frac{\partial \Lambda(u)}{\partial u} \bigg|_{u=a} + \Lambda(-a - \eta) \frac{\partial \Lambda(u)}{\partial u} \bigg|_{u=-a} \right\} \bigg|_{\{\theta_j = (-1)^j a\}} + E_0$$

$$= \phi(2a) \sinh \eta \sum_{j=1}^{2N-1} \{\coth(z_j - a - \eta/2) + \coth(z_j + a - \eta/2)\}|_{\{\theta_j = (-1)^j a\}} + E_0. \tag{3.10}$$

For the system with finite size, we solve the BAEs (3.9) and obtain the solutions of zero roots. Substituting the values into (3.10), we obtain the eigenenergy of the Hamiltonian (2.1). The results are given in Table I. The eigenenergies can also be obtained by the exact numerical diagonalization. We find that the analytical results and numerical ones are consistent with each other very well. Thus, the energy (3.10) is correct.

IV. THE PATTERNS OF ZERO ROOTS

Now, we seek the general rules of the solutions of BAEs (3.9). In this paper, we consider the Hermitian

Hamiltonian, where the model parameter a is pure imaginary and the crossing parameter η is real or $\eta \in \mathbb{R} + i\pi$. We fix the imaginary part of the zero roots in the interval $[-\pi/2, \pi/2)$ because of the periodicity property (3.7). Without losing generality, we set the imaginary parameter a as $a = ib$ and b is real. From the construction of integrable Hamiltonian (2.1), we know that the inhomogeneous parameters $\{\theta_j\}$ are pure imaginary. In this case, the crossing relation (2.9) leads to

$$R_{0,j}^{*\dagger_j}(u - \theta_j) = -\sigma_0^y R_{0,j}(-u^* - \eta - \theta_j)\sigma_0^y. \tag{4.1}$$

Substituting the above equation into Eq. (2.16), we obtain

$$t^{\dagger}(u) = (-1)^{2N-1} t(-u^* - \eta), \qquad (4.2)$$

which gives

$$\Lambda(u) = (-1)^{2N-1} \Lambda^*(-u^* - \eta). \qquad (4.3)$$

Then, we conclude that if the complex number z_j is a root of the BAEs, the $-z_j^*$ must be another root. Thus, the zero roots form the pairing solutions which have the same imaginary part but the real parts are opposite, i.e.,

$$\mathrm{Re}(z_j) + \mathrm{Re}(z_l) = 0, \qquad \mathrm{Im}(z_j) = \mathrm{Im}(z_l). \qquad (4.4)$$

The zero roots are distributed symmetrically about the imaginary axis.

The more detailed distribution of zero roots could be obtained with the help of Bethe roots. The functional identity (3.5) allows us to parametrize the eigenvalue $\Lambda(u)$ as the inhomogeneous $T - Q$ relation [25],

$$\Lambda(u)Q(u) = e^u a(u)Q(u - \eta) - e^{-u-\eta} d(u)Q(u + \eta)$$
$$\qquad\qquad - c(u)a(u)d(u), \qquad (4.5)$$

where the $Q(u)$ and $c(u)$ are given by

$$Q(u) = \prod_{j=1}^{2N} \frac{\sinh(u - \lambda_j)}{\sinh \eta},$$

$$c(u) = e^{u-2N\eta+\sum_{l=1}^{2N}(\theta_l-\lambda_l)} - e^{-u-\eta-\sum_{l=1}^{2N}(\theta_l-\lambda_l)}, \qquad (4.6)$$

and $\{\lambda_j\}$ are the Bethe roots, which should satisfy the BAEs,

$$e^{\lambda_j} a(\lambda_j)Q(\lambda_j - \eta) - e^{-\lambda_j-\eta} d(\lambda_j)Q(\lambda_j + \eta)$$
$$\qquad - c(\lambda_j)a(\lambda_j)d(\lambda_j) = 0, \quad j = 1, \dots, 2N. \qquad (4.7)$$

Putting $\lambda_j = iu_j - \eta/2$ and taking the stagger limit $\theta_j = (-1)^j a$, we rewrite the above BAEs as

$$e^{iu_j} \frac{\sin^N(u_j + b - \frac{1}{2}i\eta)\sin^N(u_j - b - \frac{1}{2}i\eta)}{\sin^N(u_j + b + \frac{1}{2}i\eta)\sin^N(u_j - b + \frac{1}{2}i\eta)}$$
$$= e^{-iu_j} \prod_{l=1}^{2N} \frac{\sin(u_j - u_l - i\eta)}{\sin(u_j - u_l + i\eta)} + 2ie^{-N\eta} \sin\left(u_j - \sum_{l=1}^{2N} u_l\right)$$
$$\times \frac{\sin^N(u_j + b - \frac{1}{2}i\eta)\sin^N(u_j - b - \frac{1}{2}i\eta)}{\prod_{l=1}^{2N} \sin(u_j - u_l + i\eta)},$$
$$j = 1, \dots, 2N. \qquad (4.8)$$

When η is positive real, for a complex u_j with a negative imaginary part, we have

$$\left|\sin\left(u_j \pm b - \frac{1}{2}i\eta\right)\right| > \left|\sin\left(u_j \pm b + \frac{1}{2}i\eta\right)\right|. \qquad (4.9)$$

This indicates that the module of the left-hand side of BAEs (4.8) tends to infinity exponentially when $N \to \infty$. To keep the equality, the denominator of the right-hand side of BAEs (4.8) must tend to zero in this limit, which gives that $u_j - u_l + i\eta \to 0$. From the $T - Q$ relation (4.5), we know that the zero roots $\{z_j - \frac{\eta}{2}\}$ and $\{iu_j - \frac{\eta}{2}\}$ of the term $\Lambda(u)Q(u)$ are undistinguishable, so $\{u_j\}$ are symmetric about the real axis since $\{z_j\}$ are symmetric about the imaginary axis from (4.4). Therefore, the general complex solutions of the Bethe roots form strings,

$$u_j = u_{j0} + i\eta\left(\frac{n+1}{2} - j\right) + o(e^{-\delta N}), \quad j = 1, \dots, n, \qquad (4.10)$$

where u_{j0} indicates the position of the n string in the real axis and $o(e^{-\delta N})$ stands for a small finite size correction.

Now we can determine the pattern of zero roots $\{z_j\}$. Putting $z_j = ix_j$ and taking the zero root $ix_j - \frac{\eta}{2}$ into Eq. (4.5), we obtain

$$e^{ix_j} \frac{\sin^N(x_j + b - \frac{1}{2}i\eta)\sin^N(x_j - b - \frac{1}{2}i\eta)}{\sin^N(x_j + b + \frac{1}{2}i\eta)\sin^N(x_j - b + \frac{1}{2}i\eta)}$$
$$= e^{-ix_j} \prod_{l=1}^{2N} \frac{\sin(x_j - u_l - i\eta)}{\sin(x_j - u_l + i\eta)} + 2ie^{-N\eta} \sin\left(x_j - \sum_{l=1}^{2N} u_l\right)$$
$$\times \frac{\sin^N(x_j + b - \frac{1}{2}i\eta)\sin^N(x_j - b - \frac{1}{2}i\eta)}{\prod_{l=1}^{2N} \sin(x_j - u_l + i\eta)},$$
$$j = 1, \dots, 2N. \qquad (4.11)$$

A similar discussion can then proceed. For the x_j with a negative imaginary part, the Eq. (4.11) leads to the relation between the zero root and Bethe root as $x_j - u_l + i\eta \to 0$ when N tends to infinity. One should note that the two sets of roots could not be equal, and the zero roots are lower in the complex plane than the Bethe roots. Combined with the fact that the $\{x_j\}$ are symmetric about the real axis from (4.4), we arrive at the similar statement that, for x_i with a positive imaginary part, $x_i - u_k - i\eta \to 0$ with $N \to \infty$ and the corresponding zero roots are higher in the complex plane than the Bethe roots. Thus, the above analysis determines the pattern of zero roots $\{x_j\}$ as

$$\mathrm{Im}(x_j) = \pm\frac{1+n}{2}\eta + o(e^{-\delta N}), \quad n = 1, 2, \dots. \qquad (4.12)$$

Substituting them into $z_j = ix_j$, we obtain

$$\mathrm{Re}(z_j) = \pm \frac{1+n}{2}\eta + o(e^{-\delta N}), \quad n = 1, 2, \ldots. \quad (4.13)$$

The above conclusion also holds for $\eta \in \mathbb{R} + i\pi$ by replacing η with $\mathrm{Re}(\eta)$.

V. THE NEARLY DEGENERATE STATES

By carefully analyzing the energy spectrum, we find an interesting phenomenon: some nearly degenerate states exist in the regime of $\eta \in \mathbb{R}$, where the NN couplings among the z direction are ferromagnetic. The energy spectrum is shown in Fig. 2(a). One sees that the energy levels can be divided into two parts. There is a big gap between the lower and upper energy levels. Further analysis gives that the patterns of zero points in these two regimes are different. In the lower regime, all the zero roots are pure imaginary and are asymmetric around the origin. The related states are the nearly degenerate states.

From the numerical results of the system with finite size, we find that there are $4N$ sets of zero roots lying on the imaginary axis, in which two sets correspond to the ground states. The other $4N - 2$ sets correspond to the nearly degenerate states. The degeneracy of the ground state is 2. In Fig. 2(b), we show the patterns of zero roots in the nearly degenerate states. Because all the zero roots are located on the imaginary axis, it is not necessary to show them in the complex plane. Thus, we choose the lateral axis of Fig. 2(b) as the energy difference $\Delta E = E_d - E_{1g}$ instead of the real axis, where E_d is the energy of nearly degenerate state and E_{1g} is the ground state energy.

To further investigate the physical properties of the nearly degenerate states, we calculate the spin texture of these states by the exact numerical diagonalization. Table II shows that the ground states and the nearly degenerate states can be regarded as the superpositions of domain walls or kinks, which are generated by continuously flipping some spins from the all spin-up state (or the all spin-down state), while the high excited states can not be.

The low-lying states, i.e., the ground and nearly degenerate states, have two domain walls. One is fixed between sites $2N$ and 1 due to the antiperiodic boundary. The other can be located between sites j and $j + 1$. This in total gives $2 \times 2N$ configurations. Subtracting two degenerated ground states, we have $4N - 2$ nearly degenerate states, which is consistent with the numerical results.

Now, we consider the relation between the nearly degenerate states and the interactions. Define $\Delta E_{\max} = \max(E_d) - E_{1g}$, where $\max(E_d)$ is the maximal energy of the nearly degenerate states and E_{1g} is the ground state energy. The energy difference $\Delta E_{\max}$ versus the model parameter $a = ib$ is shown in Fig. 2(c). From it, we see that the $\Delta E_{\max}$ changes with the changing of NN, NNN, and chiral three-spin interactions and reaches its minimum at the point of $a = i\pi/4$.

Last, we shall note that the gaps among the nearly degenerate states tend to zero with the increasing of system size. In the thermodynamic limit, these nearly degenerate states become the ground state.

VI. THERMODYNAMIC LIMIT WITH $\eta \in \mathbb{R}$

Since we have known the zero roots distribution of the BAEs, it is now possible to calculate the physical quantities in the thermodynamic limit. Based on the $t - \theta$ scheme proposed in [35,36], we choose the inhomogeneity parameters $\{\theta_j\}$ as auxiliary ones to calculate the physical quantities such as the ground state energy and the elementary excitations of the system. We first consider the regime of η is real. From the previous derivation, we know that $\{\theta_j\}$ are imaginary because that a is imaginary.

A. The ground state

At the ground state, all roots $\{z_j\}$ take imaginary values for the imaginary $\{\theta_j\}$. It is convenient to put $\theta_j = i\phi_j$ and $z_j = ix_j$, where ϕ_j and x_j take real values. Taking the
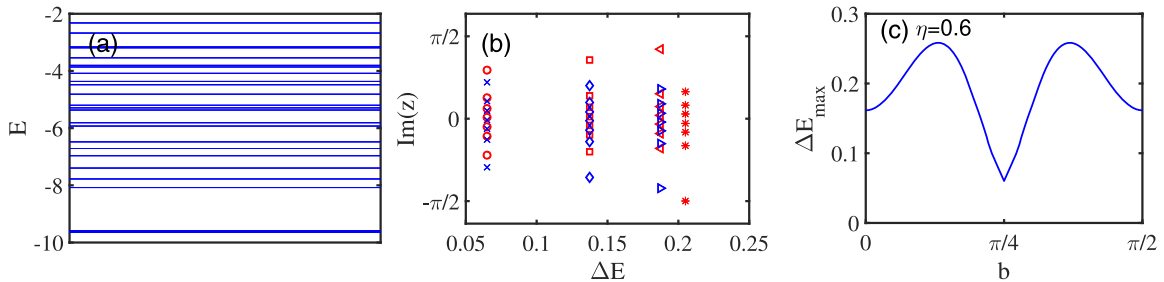

FIG. 2. (a) The system's energy levels with $2N = 8$, $b = 0.2$, and $\eta = 0.8$, where we have omitted some levels at high excited states. (b) The distribution of zero root at the nearly degenerate states for different energy difference ΔE with $2N = 8$, $b = 0.2$, and $\eta = 0.6$. There are 14 nearly degenerate states and 7 energy differences. The set of solutions of zero roots are denoted by different colors. For example, considering the double degeneracy, there are $(4N - 2)/2 = 7$ sets of different zero roots for the nearly degenerate states at $2N = 8$ case. We plot the seven sets of zero roots with different colors in Fig. 2(b) for a clearer explanation. (c) The energy difference between the highest nearly degenerate state and the ground state $\Delta E_{\max}$ versus the model parameter a with $2N = 8$ and $\eta = 0.6$.

TABLE II. The projections $\alpha_{ij} = \langle F_j | \psi_i \rangle$ and the error $\delta \equiv \| \psi_i \rangle - \sum_{j=1}^{8} \alpha_{ij} | F_j \rangle \|$ with $2N = 4$, $a = 0.2i$, and $\eta = 2$. Here, $\{ |\psi_i \rangle, i = 1, …, 16 \}$ are the eigenstates. Among them, the first two are the ground states, from the third to the eighth are the nearly degenerate states, and the rest ones are the high excited states. $\{ |F_j\rangle = \prod_{k=1}^{j-1} \sigma_{(k-1)mod(4)+1}^{x} |\uparrow\uparrow\uparrow\uparrow\rangle, j = 1, …, 8 \}$ are the approximate basis vectors of eight-dimensional low-lying states. The values of δ at the low-lying states are much smaller than those at the high excited states.

α_{ij}	$j = 1$	$j = 2$	$j = 3$	$j = 4$
$i = 1$	$0.0087 - 0.0000i$	$0.4718 - 0.1416i$	$0.0087 - 0.0000i$	$0.4718 - 0.1416i$
$i = 2$	$0.4926 + 0.0000i$	$-0.0083 + 0.0025i$	$0.4926 + 0.0000i$	$-0.0083 + 0.0025i$
$i = 3$	$-0.0000 - 0.0000i$	$0.1609 + 0.5121i$	$-0.0041 + 0.2356i$	$0.1343 - 0.3603i$
$i = 4$	$-0.0000 + 0.0000i$	$0.0742 - 0.4350i$	$-0.1622 + 0.1233i$	$0.3358 - 0.3775i$
$i = 5$	$-0.0003 - 0.0000i$	$0.0865 - 0.0343i$	$-0.4582 + 0.4296i$	$-0.2278 + 0.1911i$
$i = 6$	$-0.7011 - 0.0000i$	$-0.0000 + 0.0000i$	$0.0002 - 0.0002i$	$0.0001 - 0.0001i$
$i = 7$	$0.0030 + 0.0000i$	$-0.4606 + 0.1871i$	$-0.0030 - 0.0000i$	$0.4606 - 0.1871i$
$i = 8$	$0.4972 + 0.0000i$	$0.0028 - 0.0011i$	$-0.4972 - 0.0000i$	$-0.0028 + 0.0011i$
$i = 9$	$-0.0045 + 0.0000i$	$-0.0826 + 0.0198i$	$-0.0045 + 0.0000i$	$-0.0826 + 0.0198i$
$i = 10$	$0.0850 + 0.0000i$	$-0.0044 + 0.0011i$	$0.0850 - 0.0000i$	$-0.0044 + 0.0011i$
$i = 11$	$-0.0038 - 0.0000i$	$0.0210 + 0.0302i$	$0.0431 - 0.0244i$	$-0.0660 - 0.0173i$
$i = 12$	$0.0900 + 0.0000i$	$0.0064 + 0.0065i$	$0.0139 + 0.0033i$	$0.0056 + 0.0079i$
$i = 13$	$0.0191 - 0.0000i$	$-0.0258 - 0.0244i$	$-0.0568 - 0.0203i$	$-0.0395 - 0.0406i$
$i = 14$	$-0.0000 - 0.0000i$	$0.0715 + 0.0259i$	$-0.0400 + 0.0240i$	$0.0054 - 0.0222i$
$i = 15$	$0.0529 + 0.0000i$	$0.0043 + 0.0003i$	$-0.0529 - 0.0000i$	$-0.0043 - 0.0003i$
$i = 16$	$-0.0043 - 0.0000i$	$0.0528 + 0.0034i$	$0.0043 - 0.0000i$	$-0.0528 - 0.0034i$

$j = 5$	$j = 6$	$j = 7$	$j = 8$	δ
0.0087	$0.4718 - 0.1416i$	$0.0087 + 0.0000i$	$0.4718 - 0.1416i$	0.1702
0.4926	$-0.0083 + 0.0025i$	$0.4926 - 0.0000i$	$-0.0083 + 0.0025i$	0.1702
0.0000	$-0.1609 - 0.5121i$	$0.0041 - 0.2356i$	$-0.1343 + 0.3603i$	0.1302
0.0000	$-0.0742 + 0.4350i$	$0.1622 - 0.1233i$	$-0.3358 + 0.3775i$	0.1302
0.0003	$-0.0865 + 0.0343i$	$0.4582 - 0.4296i$	$0.2278 - 0.1911i$	0.1302
0.7011	$0.0000 - 0.0000i$	$-0.0002 + 0.0002i$	$-0.0001 + 0.0001i$	0.1302
0.0030	$-0.4606 + 0.1871i$	$-0.0030 + 0.0000i$	$0.4606 - 0.1871i$	0.1062
0.4972	$0.0028 - 0.0011i$	$-0.4972 + 0.0000i$	$-0.0028 + 0.0011i$	0.1062
-0.0045	$-0.0826 + 0.0198i$	$-0.0045 - 0.0000i$	$-0.0826 + 0.0198i$	0.9854
0.0850	$-0.0044 + 0.0011i$	$0.0850 + 0.0000i$	$-0.0044 + 0.0011i$	0.9854
0.0038	$-0.0210 - 0.0302i$	$-0.0431 + 0.0244i$	$0.0660 + 0.0173i$	0.9915
-0.0900	$-0.0064 - 0.0065i$	$-0.0139 - 0.0033i$	$-0.0056 - 0.0079i$	0.9915
-0.0191	$0.0258 + 0.0244i$	$0.0568 + 0.0203i$	$0.0395 + 0.0406i$	0.9915
0.0000	$-0.0715 - 0.0259i$	$0.0400 - 0.0240i$	$-0.0054 + 0.0222i$	0.9915
0.0529	$0.0043 + 0.0003i$	$-0.0529 - 0.0000i$	$-0.0043 - 0.0003i$	0.9943
-0.0043	$0.0528 + 0.0034i$	$0.0043 - 0.0000i$	$-0.0528 - 0.0034i$	0.9943

logarithm and considering the thermodynamic limit $N \to \infty$ of Eq. (3.9), we obtain

$$\ln |\Lambda_0^2| + 2N \int \beta_1(\phi - x)\rho(x)dx = \ln |\sinh^{-4N} \eta|$$
$$+ 2N \int \beta_2(\phi - x)\sigma(x)dx, \tag{6.1}$$

where $\beta_n(x) = \ln[\sin(x - in\eta/2)\sin(x + in\eta/2)]$, $\rho(x)$, and $\sigma(x)$ are the density of $\{x_j\}$ and $\{\phi_j\}$, respectively. Taking the derivative of Eq. (6.1) with respect to ϕ, we have

$$\int_{-\frac{\pi}{2}}^{\frac{\pi}{2}} b_1(\phi - x)\rho(x)dx = \int_{-\frac{\pi}{2}}^{\frac{\pi}{2}} b_2(\phi - x)\sigma(x)dx, \tag{6.2}$$

in which $b_n(x) = 2 \sin(2x)/[(\cos n\eta - \cos 2x)]$. Introduce the Fourier transformation,

$$f(x) = \frac{1}{\pi} \sum_{\omega = -\infty}^{+\infty} \tilde{f}(\omega)e^{i2\omega x}, \qquad \tilde{f}(\omega) = \int_{-\frac{\pi}{2}}^{\frac{\pi}{2}} f(x)e^{-i2\omega x}dx. \tag{6.3}$$

The Fourier transformation of Eq. (6.2) reads

$$\tilde{b}_1(\omega)\tilde{\rho}(\omega) = \tilde{b}_2(\omega)\tilde{\sigma}(\omega), \tag{6.4}$$

where $\tilde{b}_n(\omega) = -i2\pi \, sign(\omega)e^{-n\eta|\omega|}$. Because the total number for zero roots $\{z_j\}$ is $2N - 1$, the normalization of zero

roots density $\rho(x)$ should satisfy $\int_{-\frac{\pi}{2}}^{\frac{\pi}{2}}\rho(x)dx = \frac{2N-1}{2N}$. In the thermodynamic limit, the density of inhomogeneous parameters $\{\theta_j = (-1)^j a, j = 1, \ldots, 2N\}$ becomes $\sigma(x) = \frac{1}{2}[\delta(x-b) + \delta(x+b)]$. Taking the Fourier transformation of $\sigma(x)$, we obtain $\tilde{\sigma}(\omega) = \frac{1}{2}(e^{i2\omega b} + e^{-i2\omega b})$. Therefore, the solution of zero roots density is

$$\tilde{\rho}(\omega) = \begin{cases} e^{-\eta|\omega|}\cos(2\omega b), & \omega = \pm 1, \pm 2, \ldots, \pm\infty, \\ 1 - \frac{1}{2N}, & \omega = 0. \end{cases} \quad (6.5)$$

Taking the inverse Fourier transformation, we obtain

$$\rho(x) = \frac{1}{\pi}\left\{\frac{1 - e^{-\eta}\cos(2x + 2b)}{1 - 2e^{-\eta}\cos(2x + 2b) + e^{-2\eta}} \right.$$
$$\left. + \frac{1 - e^{-\eta}\cos(2x - 2b)}{1 - 2e^{-\eta}\cos(2x - 2b) + e^{-2\eta}}\right\}$$
$$- \frac{1}{\pi} - \frac{1}{2N\pi}. \quad (6.6)$$

The ground state energy can be calculated as

$$E_{1g} = 2N\phi(2a)\sinh\eta\int_{-\frac{\pi}{2}}^{\frac{\pi}{2}}[\coth(ix - ib - \eta/2)$$
$$+ \coth(ix + ib - \eta/2)]\rho(x)dx + E_0$$
$$= -2N\cosh\eta - N\frac{\cosh\eta\sin^2(2b)}{\sinh^2\eta}$$
$$+ \frac{\cosh(2\eta) - \cos(4b)}{\sinh\eta}. \quad (6.7)$$

Now, we check the correctness of the result (6.7). For the system (2.1) with a finite size, we obtain the ground state
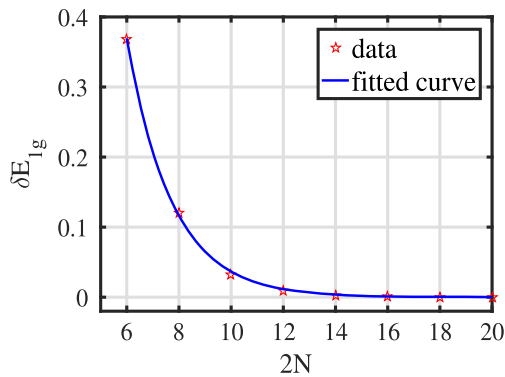

FIG. 3. The finite size scaling behavior of the quantity $\delta E_{1g} = E_{1g} - E_{1gd}$, where E_{1g} is that obtained from the analytic result (6.7) and E_{1gd} is the ground state energy calculated by the exact numerical diagonalization with finite system size. The data of δE_{1g} can be fitted as $\delta E_{1g} = 11.86e^{-0.5782\times 2N}$ with $b = 0.2$ and $\eta = 0.6$, which is exponentially decreasing and tends to zero in the thermodynamic limit.

energy E_{1gd} by using the exact diagonalization method. Define $\delta E_{1g} = E_{1g} - E_{1gd}$, where E_{1g} is the ground state energy calculated from the analytic expression (6.7). We note that both the values of E_{1gd} and δE_{1g} are dependent on the system size. Then, we take the finite size scaling analysis, and the results are shown in Fig. 3. We find that the data of δE_{1g} can be fitted as $\delta E_{1g} = 11.86e^{-0.5782\times 2N}$, where $b = 0.2$ and $\eta = 0.6$. Thus δE_{1g} is exponentially decreasing with the increasing of system size. $\delta E_{1g} \to 0$ if $N \to \infty$. Therefore, the analytic expression (6.7) gives the ground state energy in the thermodynamic limit.

B. Elementary excitation

Now we study the elementary excitation. From the general constraints of zero roots (4.4), the distribution of $\{z_j\}$ for the simplest excited state can be described by $2N - 3$ imaginary roots plus one conjugate pair. The extra conjugate paired are

$$z_{2N-2} = i\lambda + \frac{n\eta}{2} + o(e^{-\delta N}),$$
$$z_{2N-1} = i\lambda - \frac{n\eta}{2} + o(e^{-\delta N}), \quad (6.8)$$

where λ is real and $n \geq 2$. The distribution of zero roots for such an excitation with $2N = 8$ is shown in Fig. 4(a). Substituting all the zero roots into BAEs (3.9) and considering the thermodynamic limit, we obtain

$$\ln \Lambda_0^2 + 2N\int \beta_1(\phi - x)\rho(x)dx$$
$$+ \beta_{n+1}(\phi - \lambda) + \beta_{n-1}(\phi - \lambda)$$
$$= \ln(-\sinh^{-4N}\eta) + 2N\int \beta_2(\phi - x)\sigma(x)dx. \quad (6.9)$$

The derivative with respect to ϕ gives

$$2N\int_{-\frac{\pi}{2}}^{\frac{\pi}{2}} b_1(\phi - x)\rho_1(x)dx + b_{n+1}(\phi - \lambda) + b_{n-1}(\phi - \lambda)$$
$$= 2N\int_{-\frac{\pi}{2}}^{\frac{\pi}{2}} b_2(\phi - x)\sigma(x)dx. \quad (6.10)$$

Taking the Fourier transformation of (6.10), we obtain

$$2N\tilde{b}_1(\omega)\tilde{\rho}_1(\omega) + e^{-i2\omega\lambda}\tilde{b}_{n+1}(\omega) + e^{-i2\omega\lambda}\tilde{b}_{n-1}(\omega)$$
$$= 2N\tilde{b}_2(\omega)\tilde{\sigma}(\omega). \quad (6.11)$$

With the help of normalization $\int_{-\frac{\pi}{2}}^{\frac{\pi}{2}}\rho(x)dx = \frac{2N-3}{2N}$ and $\sigma(x) = \frac{1}{2}[\delta(x-b) + \delta(x+b)]$, we obtain the density of zero roots $\tilde{\rho}_1(\omega)$ as
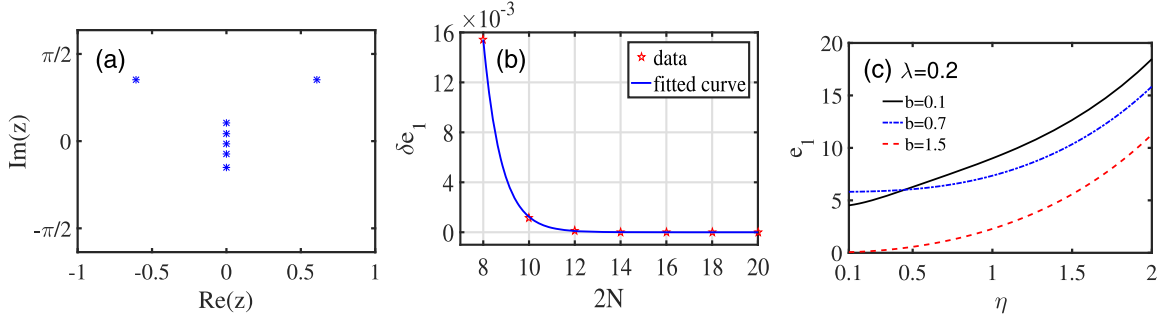
FIG. 4. (a) The distribution of zero roots at the low-lying excited state with $2N = 8$, $b = 0.2$, and $\eta = 0.6$. (b) The finite size scaling behavior of $\delta e_1 = e_1 - e_{1d}$, where e_1 is the excited energy obtained by the expression (6.14) and e_{1d} is that computed by using the exact numerical diagonalization with finite system size. Here, $b = 0.75$ and $\eta = 1$. The data can be fitted as $\delta e_1 = 376.8 e^{-1.263 \times 2N}$, which tends to zero when $N \to \infty$. (c) The excited energies with given values of b versus the anisotropic parameter η, where $n = 2$ and $\lambda = 0.2$.

$$\tilde{\rho}_1(\omega) = \begin{cases} e^{-\eta|\omega|}\cos(2\omega b) - \dfrac{e^{-i2\omega\lambda}}{2N}(e^{-n\eta|\omega|} + e^{-(n-2)\eta|\omega|}), & \omega = \pm 1, \pm 2, \ldots, \pm\infty, \\ 1 - \dfrac{3}{2N}, & \omega = 0. \end{cases} \tag{6.12}$$

The inverse Fourier transformation of $\tilde{\rho}_1(\omega)$ gives

$$\rho_1(x) = -\frac{1}{N\pi}\left\{\frac{1 - e^{-n\eta}\cos(2x - 2\lambda)}{1 - 2e^{-n\eta}\cos(2x - 2\lambda) + e^{-2n\eta}} + \frac{1 - e^{-(n-2)\eta}\cos(2x - 2\lambda)}{1 - 2e^{-(n-2)\eta}\cos(2x - 2\lambda) + e^{-2(n-2)\eta}}\right\} + \frac{1}{N\pi} + \rho(x), \tag{6.13}$$

where $\rho(x)$ is given by Eq. (6.6). Substituting the density of zero roots into Eq. (3.10), we obtain elementary excitation energy,

$$\begin{aligned} e_1(\lambda) &= 2N\phi(2a)\sinh\eta\int_{-\frac{\pi}{2}}^{\frac{\pi}{2}}[\coth(ix - ib - \eta/2) + \coth(ix + ib - \eta/2)][\rho_1(x) - \rho(x)]dx \\ &\quad + \phi(2a)\sinh\eta\left[\coth\left(\frac{n-1}{2}\eta + i\lambda - ib\right) + \coth\left(\frac{n-1}{2}\eta + i\lambda + ib\right)\right. \\ &\quad \left. + \coth\left(-\frac{n+1}{2}\eta + i\lambda - ib\right) + \coth\left(-\frac{n+1}{2}\eta + i\lambda + ib\right)\right] \\ &= \frac{\cosh(2\eta) - \cos(4b)}{\sinh\eta}\left[\frac{\sinh(n-1)\eta}{\cosh(n-1)\eta - \cos(2\lambda + 2b)} + \frac{\sinh(n-1)\eta}{\cosh(n-1)\eta - \cos(2\lambda - 2b)}\right]. \end{aligned} \tag{6.14}$$

Now, we check the correctness of Eq. (6.14). Define $\delta e_1 = e_1 - e_{1d}$, where e_1 is the excited energy obtained by the expression (6.14) and e_{1d} is that computed by using the exact numerical diagonalization with finite system size. The finite size scaling behavior of δe_1 is shown in Fig. 4(b). We see that the data can be fitted as $\delta e_1 = 376.8 e^{-1.263 \times 2N}$. In the thermodynamic limit, δe_1 tends to zero. Thus, the analytic result (6.14) is correct. The excited energies with given values of b versus the anisotropic parameter η are plotted in Fig. 4(c). We see that the excited energy increases with the increasing of η.

Substituting the distribution of zero roots (6.8) at this kind of excited state into Eq. (2.21), we obtain the momentum carried by the elementary excitation as

$$\begin{aligned} k_1(\lambda) &= -i2N\int_{-\frac{\pi}{2}}^{\frac{\pi}{2}}\ln\frac{\sinh(a + ix - \frac{\eta}{2})}{\sinh(a - ix - \frac{\eta}{2})}[\rho_1(x) - \rho(x)]dx - i\ln\frac{\sinh(a + i\lambda + \frac{n\eta}{2} - \frac{\eta}{2})\sinh(a + i\lambda - \frac{n\eta}{2} - \frac{\eta}{2})}{\sinh((a - i\lambda - \frac{n\eta}{2} - \frac{\eta}{2})\sinh(a - i\lambda + \frac{n\eta}{2} - \frac{\eta}{2})} \quad mod(2\pi) \\ &= 4\sum_{\omega=1}^{\infty}\frac{\sin(2\omega\lambda)}{\omega}\cos(2\omega b)e^{-n\eta\omega}\cosh(\eta\omega) \\ &\quad + \frac{i}{2}\left[\ln\frac{\sin(b + \lambda + i\frac{n-1}{2}\eta)\sin(b + \lambda - i\frac{n+1}{2}\eta)}{\sin(b - \lambda + i\frac{n-1}{2}\eta)\sin(b - \lambda - i\frac{n+1}{2}\eta)} - \ln\frac{\sin(b + \lambda - i\frac{n-1}{2}\eta)\sin(b + \lambda + i\frac{n+1}{2}\eta)}{\sin(b - \lambda - i\frac{n-1}{2}\eta)\sin(b - \lambda + i\frac{n+1}{2}\eta)}\right] \quad mod(2\pi). \end{aligned} \tag{6.15}$$

VII. THERMODYNAMIC LIMIT WITH $\eta \in \mathbb{R} + i\pi$

In this section, we study the physical quantities in the regime of $\eta \in \mathbb{R} + i\pi$. The patterns of zero roots of BAEs are given by Eq. (4.13) with the replacing η by $\text{Re}(\eta)$. For simplicity, we define $\eta_+ = \eta - i\pi$, then the patterns read

$$\text{Re}(z_j) = \pm \frac{1+n}{2}\eta_+ + o(e^{-\delta N}), \quad n = 1, 2, \ldots. \quad (7.1)$$

Without losing generality, we suppose $b \in (0, \pi/2)$.

A. Ground state and quantum phase transition

At the ground state, the pattern of zero roots $\{z_j\}$ includes $N - 1$ conjugate pairs and one pure imaginary solution, i.e.,

$$z_{2j-1} = ix_{2j-1} + \eta_+ + o(e^{-\delta N}), \qquad z_{2j} = ix_{2j} - \eta_+ + o(e^{-\delta N}), \quad j = 1, \ldots, N-1,$$
$$z_{2N-1} = i\mu, \quad (7.2)$$

where $\{x_j\}$ and μ are real. Substituting the pattern (7.2) into Eq. (3.9), taking the logarithm and considering the thermodynamic limit, we obtain

$$\ln|\Lambda_0^2| + \gamma_1(\phi - \mu) + 2N \int [\gamma_1(\phi - x) + \gamma_3(\phi - x)]\rho_2(x)dx$$
$$= \ln|\sinh^{-4N}\eta_+| + 2N \int \beta_2(\phi - x)\sigma(x)dz, \quad (7.3)$$

in which $\gamma_n(x) = \ln[\cos(x - in\eta_+/2)\cos(x + in\eta_+/2)]$, and $\rho_2(x)$ and $\sigma(x)$ denote the density of $\{x_j\}$ and $\{\phi_j\}$, respectively. Taking the derivative, we have

$$-c_1(\phi - \mu) - 2N \int_{-\frac{\pi}{2}}^{\frac{\pi}{2}} [c_1(\phi - x) + c_3(\phi - x)]\rho_2(x)dx = 2N \int_{-\frac{\pi}{2}}^{\frac{\pi}{2}} b_2(\phi - x)\sigma(x)dx, \quad (7.4)$$

where $c_n(x) = \tan(x + in\eta_+/2) + \tan(x - in\eta_+/2)$. The Fourier transformation of Eq. (7.4) gives

$$-e^{-i2\omega\mu}\tilde{c}_1(\omega) - 2N[\tilde{c}_1(\omega) + \tilde{c}_3(\omega)]\tilde{\rho}_2(\omega) = 2N\tilde{b}_2(\omega)\tilde{\sigma}(\omega), \quad (7.5)$$

where $\tilde{c}_n(\omega) = (-1)^\omega sign(\omega)2\pi i e^{-n\eta|\omega|}$. With the help of normalization $\int_{-\frac{\pi}{2}}^{\frac{\pi}{2}} \rho(x)dx = \frac{1}{2} - \frac{1}{2N}$, we obtain the solution of zero roots density,

$$\tilde{\rho}_2(\omega) = \begin{cases} -\frac{\frac{1}{2N}e^{-i2\omega\mu} - (-1)^\omega e^{-\eta_+|\omega|}\cos(2\omega b)}{1 + e^{-2\eta_+|\omega|}}, & \omega = \pm 1, \pm 2, \ldots, \pm\infty, \\ \frac{1}{2} - \frac{1}{2N}, & \omega = 0. \end{cases} \quad (7.6)$$

Then, the ground state energy is

$$E(\mu) = 2N\phi(2a)\sinh\eta \int_{-\frac{\pi}{2}}^{\frac{\pi}{2}} [\coth(ix + \eta_+ - ib - \eta/2) + \coth(ix - \eta_+ - ib - \eta/2)$$
$$+ \coth(ix + \eta_+ + ib - \eta/2) + \coth(ix - \eta_+ + ib - \eta/2)]\rho_2(x)dx$$
$$+ \phi(2a)\sinh\eta[\coth(i\mu - ib - \eta/2) + \coth(i\mu + ib - \eta/2)] + E_0.$$
$$= -4N\frac{\cosh(2\eta_+) - \cos(4b)}{\sinh\eta_+} \sum_{\omega=1}^{\infty} e^{-2\eta_+\omega}\cos^2(2b\omega)\tanh(\eta_+\omega) + 2\frac{\cosh(2\eta_+) - \cos(4b)}{\sinh\eta_+}$$
$$\times \sum_{\omega=1}^{\infty} (-1)^\omega e^{-\eta_+\omega}\cos(2b\omega)\cos(2\mu\omega)\tanh(\eta_+\omega) + \frac{1}{2}[\cosh(2\eta_+) - \cos(4b)]$$
$$\times \left[\frac{1}{\cosh(\eta_+) + \cos 2(\mu + b)} + \frac{1}{\cosh(\eta_+) + \cos 2(\mu - b)} \right] + \frac{N\cosh\eta_+[\cos^2(2b) - \cosh(2\eta_+)]}{\sinh^2\eta_+}. \quad (7.7)$$

Some remarks are in order. From Eq. (7.7), we see that the values of $E(\mu)$ is dependent on the strength of the boundary string μ. At the ground state, $E(\mu)$ should take its minimum. Thus, the boundary string at the ground state is fixed. We find that $E(\mu)$ arrives at its minimum at the point

of $\mu = 0$ if $b \in (0, \pi/4)$, and at the point of $\mu = -\pi/2$ if $b \in (\pi/4, \pi/2)$. This conclusion can also be achieved as follows. If $\eta_+ \to \infty$, many terms in Eq. (7.7) tend to zero. Keeping the order of $e^{-\eta_+}$, the μ-dependent terms in Eq. (7.7) can be approximated as

$$
2\frac{\cosh(2\eta_+) - \cos(4b)}{\sinh \eta_+} \sum_{\omega=1}^{\infty} (-1)^{\omega} e^{-\eta_+ \omega} \cos(2b\omega) \cos(2\mu\omega) \tanh(\eta_+ \omega)
$$

$$
+ \frac{1}{2}[\cosh(2\eta_+) - \cos(4b)]\left[\frac{1}{\cosh(\eta_+) + \cos 2(\mu + b)} + \frac{1}{\cosh(\eta_+) + \cos 2(\mu - b)}\right]
$$

$$
\approx \frac{\cosh(2\eta_+) - \cos(4b)}{\cosh \eta_+}[1 - 4e^{-\eta_+} \cos(2b) \cos(2\mu)], \tag{7.8}
$$

which has the minimum at $\mu = 0$ for $b \in (0, \pi/4)$, and at $\mu = -\pi/2$ for $b \in (\pi/4, \pi/2)$. If η_+ is finite, we have checked this conclusion numerically and find that it is true. Therefore, the ground state energy in the regime of $b \in (0, \pi/4)$ (phase I) is

$$
E_{2g} = -4N\frac{\cosh(2\eta_+) - \cos(4b)}{\sinh \eta_+} \sum_{\omega=1}^{\infty} e^{-2\eta_+ \omega} \cos^2(2b\omega) \tanh(\eta_+ \omega)
$$

$$
+ 2\frac{\cosh(2\eta_+) - \cos(4b)}{\sinh \eta_+} \sum_{\omega=1}^{\infty} (-1)^{\omega} e^{-\eta_+ \omega} \cos(2b\omega) \tanh(\eta_+ \omega)
$$

$$
+ \frac{\cosh(2\eta_+) - \cos(4b)}{\cosh(\eta_+) + \cos(2b)} + \frac{N \cosh \eta_+ [\cos^2(2b) - \cosh(2\eta_+)]}{\sinh^2 \eta_+}. \tag{7.9}
$$

The ground state energy in the regime of $b \in (\pi/4, \pi/2)$ (phase II) is

$$
E_{3g} = -4N\frac{\cosh(2\eta_+) - \cos(4b)}{\sinh \eta_+} \sum_{\omega=1}^{\infty} e^{-2\eta_+ \omega} \cos^2(2b\omega) \tanh(\eta_+ \omega)
$$

$$
+ 2\frac{\cosh(2\eta_+) - \cos(4b)}{\sinh \eta_+} \sum_{\omega=1}^{\infty} e^{-\eta_+ \omega} \cos(2b\omega) \tanh(\eta_+ \omega)
$$

$$
+ \frac{\cosh(2\eta_+) - \cos(4b)}{\cosh(\eta_+) - \cos(2b)} + \frac{N \cosh \eta_+ [\cos^2(2b) - \cosh(2\eta_+)]}{\sinh^2 \eta_+}. \tag{7.10}
$$

Now, we check the correctness of analytical expressions (7.9) and (7.10). The zero roots distributions with $2N = 8$ are shown in Fig. 5(a). The finite size scaling behavior of $\delta E_{2g} = E_{2g} - E_{2gd}$ is shown in Fig. 5(b), where E_{2g} is the analytical result obtained by Eq. (7.9) and E_{2gd} is the one calculated by the exact numerical diagonalization. The data can be fitted as $\delta E_{2g} = 4.076 \times (2N)^{-1.032}$. Thus, δE_{2g} tends to zero in the thermodynamic limit. The numerical results and the analytical ones agree with each other very well. The ground state energies versus the model parameter b are shown in Fig. 5(c), where the red dots are the numerical data with $2N = 18$ and the blue solid lines are the analytical data. The derivative of the ground state energies versus the

interaction b is shown in Fig. 5(d). From it, we see that the ground state energies are continuous and their derivatives are discontinuous. Thus, there exists a first order quantum phase transition at the critical point $b = \pi/4$.

B. Elementary excitation I

In the regime of $\eta \in \mathbb{R} + i\pi$, the system has two kinds of elementary excitations. The first kind of excitation is characterized by the root $i\mu$ sliding along the imaginary axis in the interval $[-i\pi/2, i\pi/2)$ but away from the points of 0 and $-i\pi/2$. In the regime of $b \in (0, \pi/4)$, the excited energy is
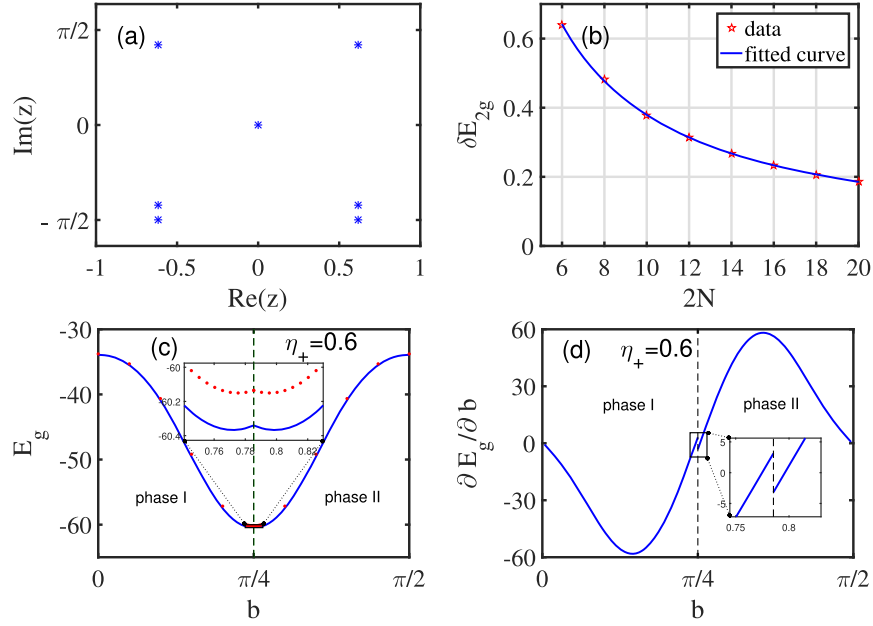
FIG. 5.   The distribution of zero roots $\{z_j\}$ at the ground states with $2N = 8$, $\eta_+ = 0.6$, and $b = 0.2$. (b) The finite size scaling behavior of $\delta E_{2g} = E_{2g} - E_{2gd}$ with $\eta_+ = 0.6$ and $b = 0.2$. Here, E_{2g} is the analytical result obtained by Eq. (7.9) and E_{2gd} is the one calculated by the exact numerical diagonalization. The data can be fitted as $\delta E_{2g} = 4.076 \times (2N)^{-1.032}$. Thus, δE_{2g} tends to zero in the thermodynamic limit. (c) The ground state energy versus the interaction b, where the blue solid line is the analytical result and red dots are the numerical ones with $2N = 18$. Comparing the blue solid line and red dots, we see that the finite size scaling effect at $2N = 18$ is small. (d) The derivative of ground state energy against the interaction b. At the point of $b = \pi/4$, the derivative is discontinuous.

$$e_2(\mu) = 2\frac{\cosh(2\eta_+) - \cos(4b)}{\sinh\eta_+}\sum_{\omega=1}^{\infty}(-1)^\omega e^{-\eta_+\omega}[\cos(2\mu\omega) - 1]\cos(2b\omega)\tanh(\eta_+\omega)$$

$$+ \frac{1}{2}[\cosh(2\eta_+) - \cos(4b)]\left[\frac{1}{\cosh(\eta_+) + \cos 2(\mu + b)} + \frac{1}{\cosh(\eta_+) + \cos 2(\mu - b)} - \frac{2}{\cosh(\eta_+) + \cos(2b)}\right]. \quad (7.11)$$

The corresponding momentum is

$$k_2(\mu) = -i2N\int_{-\frac{\pi}{2}}^{\frac{\pi}{2}}\ln\frac{\cos(b + x - i\frac{\eta_+}{2})\cos(b + x + i\frac{3\eta_+}{2})}{\cos(b - x - i\frac{\eta_+}{2}))\cos(b - x + i\frac{3\eta_+}{2})}[\rho_2(\mu, x) - \rho_2(\mu = 0, x)]dx - i\ln\frac{\cos(b + \mu + i\frac{\eta_+}{2})}{\cos(b - \mu + i\frac{\eta_+}{2})}mod(2\pi)$$

$$= 2\sum_{\omega=1}^{\infty}\frac{\sin(2\omega\mu)}{\omega}\cos(2\omega b)e^{-\eta_+\omega}\tanh(\eta_+\omega) + \frac{i}{2}\left[\ln\frac{\cos(b + \mu - i\frac{\eta_+}{2})}{\cos((b - \mu - i\frac{\eta_+}{2})} - \ln\frac{\cos(b + \mu + i\frac{\eta_+}{2})}{\cos(b - \mu + i\frac{\eta_+}{2})}\right]mod(2\pi). \quad (7.12)$$

Now, we check the corrections of Eqs. (7.11) and (7.12). The excited energy e_2 and the associated momentum k_2 versus the boundary string μ are demonstrated in Fig. 6(a), where the blue dash-dotted line and the black dash line are the analytical results calculated from Eqs. (7.11) and (7.12), and the red stars and circles are the numerical data obtained by exactly diagonalizing the system with $2N = 10$. From them, we see that the analytic expressions are in good agreement with the numerical results. The finite size scaling behavior of the energy difference $\delta e_2 = e_2 - e_{2d}$ is shown in Fig. 6(b), where e_2 is the analytical result

obtained by Eq. (7.11) and e_{2d} is the numerical one. The data can be fitted as $\delta e_2 = 0.2658 \times e^{-0.125 \times 2N}$, which tends to zero when N tends to infinite. Thus, the result (7.11) is correct. The excited energies with given values of interaction b versus the anisotropic parameter η_+ are plotted in Fig. 6(c). We see that if the interaction b is small, the excited energies are increasing with the increasing of η_+. While if b is large, the excited energies have a maximum at a suitable value of η_+. The dispersion relations between e_2 and k_2 with give b are shown in Fig. 6(d). From it, we see that the excitation is gapless.
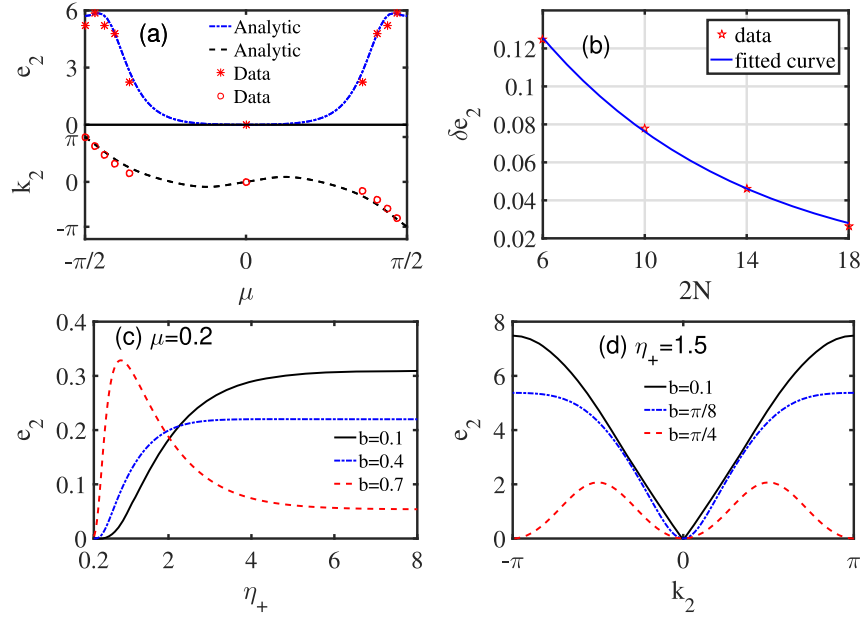
FIG. 6. The gapless excitation in the antiferromagnetic phase I. (a) The excited energy e_2 and the momentum k_2 versus the string strength μ. The blue solid line is the excited energy calculated from Eq. (7.11), the black solid line is the momentum obtained from Eq. (7.12), and the red circles and starts are the numerical results computed by using the exact diagonalization with $2N = 10$, where $b = 0.2$ and $\eta_+ = 0.6$. The slight differences are due to the finite size corrections. (b) The finite size scaling behavior of $\delta e_2 = e_2 - e_{2d}$ with $\eta_+ = 1$ and $b = 0.75$. Here, e_2 is the analytical result obtained by Eq. (7.11), and e_{2d} is the numerical datum with finite system size. The data can be fitted as $\delta e_2 = 0.2658 \times e^{-0.125 \times 2N}$, which tends to zero in the thermodynamic limit. (c) The excited energy e_2 as a function of anisotropic parameter η_+ with $\mu = 0.2$ and $b = 0.1, 0.4, 0.7$. (d) The dispersion relation of the first kind of elementary excitation in the phase I with $\eta_+ = 1.5$ and $b = 0.1, \pi/8, \pi/4$.

In the regime of $b \in (\pi/4, \pi/2)$, the excited energy is

$$e_3(\mu) = 2 \frac{\cosh(2\eta_+) - \cos(4b)}{\sinh \eta_+} \sum_{\omega=1}^{\infty} e^{-\eta_+ \omega}[(-1)^\omega \cos(2\mu\omega) - 1]\cos(2b\omega)\tanh(\eta_+ \omega)$$

$$+ \frac{1}{2}[\cosh(2\eta_+) - \cos(4b)]\left[\frac{1}{\cosh(\eta_+) + \cos 2(\mu+b)} + \frac{1}{\cosh(\eta_+) + \cos 2(\mu-b)} - \frac{2}{\cosh(\eta_+) - \cos(2b)}\right]. \quad (7.13)$$

The associated momentum is

$$k_3(\mu) = k_2(\mu) + \pi \quad mod(2\pi). \quad (7.14)$$

The correctness of Eq. (7.13) is demonstrated by the finite size scaling behavior of $\delta e_3 = e_3 - e_{3d}$ shown in Fig. 7(a), where e_2 is the excited energy obtained from Eq. (7.13) and
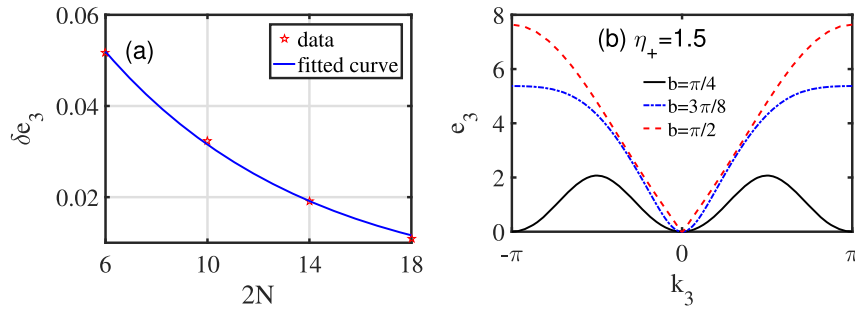

FIG. 7. The gapless excitation in the antiferromagnetic phase II. (a) The finite size scaling behavior of $\delta e_3 = e_3 - e_{3d}$ with $\eta_+ = 1$ and $b = 0.8$. Here, e_3 is the analytical result obtained by Eq. (7.13), and e_{3d} is the numerical one. The data can be fitted as $\delta e_3 = 0.1097 \times e^{-0.1247 \times 2N}$, which is zero in the thermodynamic limit. (b) The dispersion relation of the first kind of elementary excitation in the phase II with $\eta_+ = 1.5$ and $b = \pi/4, 3\pi/8, \pi/2$.

TABLE III. The projections $\beta_{ij} = \langle N_j | \psi_i \rangle$ and the error $\bar{\delta} = \| |\psi_i\rangle - \sum_{j=1}^{8} \beta_{ij} |N_j\rangle \|$ with $2N = 4$, $a = 0.2i$, and $\eta_+ = 2$. Here $\{|\psi_i\rangle, i = 1, \ldots, 16\}$ are the eigenstates. Among them, the first two are the ground states, from the third to the eighth are the type I low-lying excited states, and the rest ones are the high excited states. $\{|N_j\rangle = \prod_{k=1}^{j-1} \sigma_{(k-1)mod(4)+1}^x |\uparrow\downarrow\uparrow\downarrow\rangle, j = 1, \ldots, 8\}$ are the approximate basis vectors of eight-dimensional low-lying states. The values of $\bar{\delta}$ at the low-lying states are much smaller than those at the high excited states.

β_{ij}	$j=1$	$j=2$	$j=3$	$j=4$	$j=5$	$j=6$	$j=7$	$j=8$	$\bar{\delta}$
$i=1$	$0.4972 - 0.0000i$	$-0.0000 + 0.0000i$	0.4972	$-0.0000 + 0.0000i$	$0.4972 - 0.0000i$	$-0.0000 + 0.0000i$	$0.4972 + 0.0000i$	$-0.0000 + 0.0000i$	0.1062
$i=2$	$0.2300 + 0.1375i$	$0.4188 + 0.0000i$	$0.2300 + 0.1375i$	0.4188	$0.2300 + 0.1375i$	$0.4188 + 0.0000i$	$0.2300 + 0.1375i$	$0.4188 + 0.0000i$	0.1062
$i=3$	$-0.1834 - 0.2577i$	$-0.4905 - 0.0000i$	$0.2971 - 0.2132i$	$0.1231 - 0.0456i$	$0.1834 + 0.2577i$	0.4905	$-0.2971 + 0.2132i$	$-0.1231 + 0.0456i$	0.1302
$i=4$	$-0.2413 - 0.1058i$	$-0.2207 - 0.3389i$	$-0.4955 + 0.0000i$	$0.1003 - 0.0541i$	$0.2413 + 0.1058i$	$0.2207 + 0.3389i$	0.4955	$-0.1003 + 0.0541i$	0.1302
$i=5$	$0.0703 + 0.0084i$	$-0.0999 - 0.3037i$	$0.0599 + 0.0260i$	$-0.6164 - 0.0000i$	$-0.0703 - 0.0084i$	$0.0999 + 0.3037i$	$-0.0599 - 0.0260i$	0.6164	0.1302
$i=6$	$-0.1425 - 0.1667i$	$0.2350 + 0.3183i$	$-0.0877 + 0.0745i$	0.5231	$0.1425 + 0.1667i$	$-0.2350 - 0.3183i$	$0.0877 - 0.0745i$	$-0.5231 + 0.0000i$	0.1302
$i=7$	$-0.4927 + 0.0000i$	$0.0000 - 0.0000i$	0.4927	$-0.0000 + 0.0000i$	$-0.4927 + 0.0000i$	$-0.0000 - 0.0000i$	0.4927	$-0.0000 + 0.0000i$	0.1702
$i=8$	$0.0450 + 0.0186i$	0.4903	$-0.0450 - 0.0186i$	$-0.4903 - 0.0000i$	$0.0450 + 0.0186i$	$0.4903 + 0.0000i$	$-0.0450 - 0.0186i$	$-0.4903 - 0.0000i$	0.1702
$i=9$	$-0.0461 - 0.0264i$	$-0.0000 - 0.0000i$	$-0.0461 - 0.0264i$	$0.0000 + 0.0000i$	$-0.0461 - 0.0264i$	$-0.0000 - 0.0000i$	$-0.0461 - 0.0264i$	$0.0000 + 0.0000i$	0.9943
$i=10$	$0.0003 - 0.0002i$	$-0.0461 + 0.0264i$	$0.0003 - 0.0002i$	$-0.0461 + 0.0264i$	$0.0003 - 0.0002i$	$-0.0461 + 0.0264i$	$0.0003 - 0.0002i$	$-0.0461 + 0.0264i$	0.9943
$i=11$	$-0.0120 + 0.0007i$	$0.0020 - 0.0048i$	$-0.0835 - 0.0366i$	$0.0014 - 0.0002i$	$0.0120 - 0.0007i$	$-0.0020 + 0.0048i$	$0.0835 + 0.0366i$	$-0.0014 + 0.0002i$	0.9915
$i=12$	$0.0797 + 0.0350i$	$-0.0159 + 0.0149i$	$-0.0087 - 0.0102i$	$-0.0156 - 0.0030i$	$-0.0797 - 0.0350i$	$0.0159 - 0.0149i$	$0.0087 + 0.0102i$	$0.0156 + 0.0030i$	0.9915
$i=13$	$0.0102 + 0.0042i$	$-0.0788 + 0.0346i$	$-0.0023 - 0.0046i$	$0.0299 + 0.0064i$	$-0.0102 - 0.0042i$	$0.0788 - 0.0346i$	$0.0023 + 0.0046i$	$-0.0299 - 0.0064i$	0.9915
$i=14$	$0.0688 + 0.0302i$	$0.0270 - 0.0114i$	$-0.0065 - 0.0070i$	$0.0415 + 0.0130i$	$-0.0688 - 0.0302i$	$-0.0270 + 0.0114i$	$0.0065 + 0.0070i$	$-0.0415 - 0.0130i$	0.9915
$i=15$	$-0.0811 - 0.0257i$	$-0.0000 - 0.0000i$	$0.0811 + 0.0257i$	$0.0000 + 0.0000i$	$-0.0811 - 0.0257i$	$-0.0000 - 0.0000i$	$0.0811 + 0.0257i$	$0.0000 + 0.0000i$	0.9854
$i=16$	$-0.0023 - 0.0001i$	$-0.0811 + 0.0257i$	$0.0023 + 0.0001i$	$0.0811 - 0.0257i$	$-0.0023 - 0.0001i$	$-0.0811 + 0.0257i$	$0.0023 + 0.0001i$	$0.0811 - 0.0257i$	0.9854

δe_3 is the numerical one. We see that the data can be fitted as $\delta e_3 = 0.1097 \times e^{-0.1247 \times 2N}$, which is zero in the thermodynamic limit. Based on Eqs. (7.13) and (7.14), the dispersion relations in phase II are shown in Fig. 7(b). We see the excitation is also gapless in this regime.

The physical picture of this kind of elementary excitation is as follows. From Table III, we see that these excited states can be regarded as the superposition of domain walls, which are generated by continuously flipping some spins of antiferromagnetic Neel states $|\uparrow\downarrow \cdots \uparrow\downarrow\rangle$ or $|\downarrow\uparrow \cdots \downarrow\uparrow\rangle$. We should note that the gaps of this kind of states for the system with finite size do not tend to zero in the thermodynamic limit in the regime if $\eta \in \mathbb{R} + i\pi$; thus, they are not the nearly degenerate states. If the NN along x and y direction, NNN and chiral three-spin interactions

vanish, the model (2.1) reduces to the Ising model. For the Ising model, these low-lying excited states degenerate to the ground state in the thermodynamic limit. Therefore, the anisotropic NN, NNN and chiral three-spin interactions separate those excited state away from each other and preserve the finite energy difference even in the thermodynamic limit.

The competing of the anisotropic NN, NNN and chiral three-spin interactions will change these excited energies and induce the quantum phase transition. In the phase I, the NN interactions along the x and y directions are ferromagnetic. With the increasing of interaction parameter b, the energies for modes of momentum π or $-\pi$ are decreasing and eventually tend to zero; please see Fig. 6(d). If the value of b is larger than the critical point $\pi/4$, the NN interactions along

the x- and y-directions become antiferromagnetic, and the contribution of chiral three-spin interactions along the z direction also changes. The energy of π mode is lower than the ground state energy in phase I, and the corresponding state becomes the new ground state in phase II. From Fig. 6(a), we also see that the momentum π corresponds to $\mu = -\pi/2$, which determines the ground state in phase II. This result agrees with that given by Eq. (7.10). Then, we demonstrate that there exists a quantum phase transition from the phase I to

the phase II. Thus, the competition have significantly influenced this kind of low-lying gapless excitations and can induce the phase transition.

C. Elementary excitation II

The second kind of elementary excitations is quantified by a conjugate pair of z roots turning into two imaginary ones, i.e.,

$$
\begin{aligned}
&z_{2j-1} = ix_{2j-1} + \eta_+ + o(e^{-\delta N}), \qquad z_{2j} = ix_{2j} - \eta_+ + o(e^{-\delta N}), \quad j = 1, \dots, N-2, \\
&z_{2N-3} = i\mu_1 + o(e^{-\delta N}), \qquad z_{2N-2} = i\mu_2 + o(e^{-\delta N}), \\
&z_{2N-1} = i\mu,
\end{aligned}
\tag{7.15}
$$

where x_j, μ_1, μ_2, and μ are all real. The root patterns of such excitations for the phases I are shown in Fig. 8(a). Using the similar procedure mentioned above, we obtain the density of zero roots in the thermodynamic limit should satisfy the integral equation,

$$
-c_1(\phi - \mu) - c_1(\phi - \mu_1) - c_1(\phi - \mu_2) - 2N \int_{-\frac{\pi}{2}}^{\frac{\pi}{2}} [c_1(\phi - x) + c_3(\phi - x)]\rho_2(x)dx = 2N \int_{-\frac{\pi}{2}}^{\frac{\pi}{2}} b_2(\phi - x)\sigma(x)dx. \tag{7.16}
$$

With the help of Fourier transformation, we obtain the solution as

$$
\tilde{\rho}_3(\omega) = \begin{cases} -\dfrac{\frac{1}{2N}(e^{-i2\omega\mu} + e^{-i2\omega\mu_1} + e^{-i2\omega\mu_2}) - (-1)^\omega e^{-\eta_+|\omega|}\cos(2\omega b)}{1 + e^{-2\eta_+|\omega|}}, & \omega = \pm 1, \dots, \\ \dfrac{1}{2} - \dfrac{1}{N}, & \omega = 0. \end{cases}
$$

We find that the excited energies in phases I and II have the same expression,

$$
\begin{aligned}
e_4(\mu_1, \mu_2) &= E(\mu_1, \mu_2, \mu = 0) - E(\mu = 0) = E\left(\mu_1, \mu_2, \mu = -\frac{\pi}{2}\right) - E\left(\mu = -\frac{\pi}{2}\right) \\
&= \epsilon(\mu_1) + \epsilon(\mu_2),
\end{aligned}
\tag{7.17}
$$

where

$$
\begin{aligned}
\epsilon(\mu) &= 2\frac{\cosh(2\eta_+) - \cos(4b)}{\sinh\eta_+}\sum_{\omega=1}^{\infty}(-1)^k e^{-\eta_+\omega}\cos(2\mu\omega)\cos(2b\omega)\tanh(\eta_+\omega) \\
&+ \frac{1}{2}[\cosh(2\eta_+) - \cos(4b)]\left[\frac{1}{\cosh(\eta_+) + \cos 2(\mu + b)} + \frac{1}{\cosh(\eta_+) + \cos 2(\mu - b)}\right].
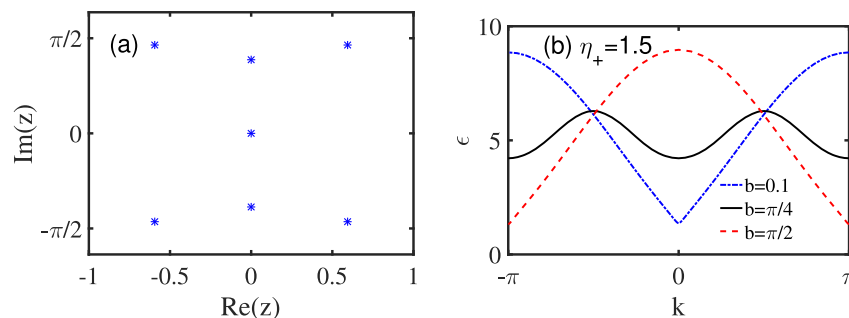\end{aligned}
\tag{7.18}
$$

FIG. 8. The gapped spinon excitations. (a) The pattern of zero roots with $2N = 8$, $\eta_+ = 0.6$, and $b = 0.2$. (b) The dispersion relations with $\eta_+ = 1.5$ and $b = 0.1$, $\pi/4$, $\pi/2$.

The corresponding momentum reads

$$
\begin{aligned}
k_4(\mu_1,\mu_2) &= -i2N \int_{-\frac{\pi}{2}}^{\frac{\pi}{2}} \ln \frac{\cos(b+x-i\frac{\eta_+}{2})\cos(b+x+i\frac{3\eta_+}{2})}{\cos(b-x-i\frac{\eta_+}{2})\cos(b-x+i\frac{3\eta_+}{2})} [\rho_3(\mu_2,\mu_1,\mu,x)-\rho_2(\mu,x)]dx \\
&\quad -i\ln\frac{\cos(b+\mu_1+i\frac{\eta_+}{2})}{\cos(b-\mu_1+i\frac{\eta_+}{2})} - i\ln\frac{\cos(b+\mu_2+i\frac{\eta_+}{2})}{\cos(b-\mu_2+i\frac{\eta_+}{2})} \quad mod(2\pi) \\
&= k_2(\mu_1)+k_2(\mu_2) \quad mod(2\pi).
\end{aligned}
\tag{7.19}
$$

From Eqs. (7.17) and (7.19), we see that both the energy and the momentum of this kind of elementary excitations depend on two free parameters. They are the typical spinon excitations. The dispersion relations with given b are shown in Fig. 8(b). We see that there always exists an energy gap and this kind of excitations is gapped.

VIII. CONCLUSIONS

In this paper, we have studied the exact physical properties of an integrable antiperiodic $J_1 - J_2$ spin chain that includes the NN, NNN, and chiral three-spin interactions in the thermodynamic limit. With the help of the inhomogeneous $T - Q$ relation, we obtain the zero roots distributions of the transfer matrix focusing on the interaction parameter where a is imaginary and η is real or $\eta \in \mathbb{R} + i\pi$. Based on the root patterns, we calculate the ground state energies, elementary excitations, and dispersion relations. We also discuss the nearly degenerate states in the ferromagnetic regime with $\eta \in \mathbb{R}$ and the quantum phase transition in the antiferromagnetic regime with $\eta \in \mathbb{R} + i\pi$. We demonstrate the competing of NN, NNN, and chiral three-spin interactions can induce many interesting phenomena.

[1] L. Onsager, Phys. Rev. **65**, 117 (1944).

[2] E. H. Lieb and F. Y. Wu, Phys. Rev. Lett. **20**, 1445 (1968).

[3] J. M. P. Carmelo and P. D. Sacramento, Phys. Rep. **749**, 1 (2018).

[4] H. Bethe, Z. Phys. **71**, 205 (1931).

[5] L. A. Takhtadzhan and L. D. Faddeev, Rush. Math. Surv. **34**, 11 (1979).

[6] L. D. Faddeev, Sov. Sci. Rev. Math. C **1**, 107 (1980).

[7] E. K. Sklyanin, L. A. Takhtajan, and L. D. Faddeev, Theor. Math. Phys. **40**, 688 (1979).

[8] E. K. Sklyanin, J. Sov. Math. **19**, 1546 (1982).

[9] P. P. Kulish and E. K. Sklyanin, Lect. Notes Phys. **151**, 61 (1982).

[10] L. A. Takhtajan, Lect. Notes Phys. **242**, 175 (1985).

[11] E. K. Sklyanin, J. Phys. A **21**, 2375 (1988).

[12] R. J. Baxter, Phys. Rev. Lett. **26**, 832 (1971).

[13] R. J. Baxter, Phys. Rev. Lett. **26**, 834 (1971).

[14] J. Cao, H. Q. Lin, K. J. Shi, and Y. Wang, Nucl. Phys. **B663**, 487 (2003).

[15] C. M. Yung and M. T. Batchelor, Nucl. Phys. **B446**, 461 (1995).

[16] R. I. Nepomechie, Nucl. Phys. **B662**, 615 (2002).

[17] P. Baseilhac, Nucl. Phys. **B754**, 309 (2006).

[18] P. Baseilhac and K. Koizumi, J. Stat. Mech. (2007) P09006.

[19] S. Niekamp, T. Wirth, and H. Frahm, J. Phys. A **42**, 195008 (2009).

[20] G. Niccoli, Nucl. Phys. **B870**, 397 (2013).

[21] S. Belliard, Nucl. Phys. **B892**, 1 (2015).

[22] S. Belliard and R. A. Pimenta, Nucl. Phys. **B894**, 527 (2015).

[23] J. Avan, S. Belliard, N. Grosjean, and R. A. Pimenta, Nucl. Phys. **B899**, 229 (2015).

[24] J. Cao, W.-L. Yang, K. Shi, and Y. Wang, Phys. Rev. Lett. **111**, 137201 (2013).

[25] Y. Wang, W.-L. Yang, J. Cao, and K. Shi, *Off-Diagonal Bethe Ansatz for Exactly Solvable Models* (Springer, Berlin, 2015).

[26] J. de Gier and F. H. L. Essler, Phys. Rev. Lett. **95**, 240601 (2005).

[27] J. Sirker, R. G. Pereira, and I. Affleck, Phys. Rev. Lett. **103**, 216602 (2009).

[28] L. Fu and C. L. Kane, Phys. Rev. Lett. **100**, 096407 (2008).

[29] R. M. Lutchyn, J. D. Sau, and S. Das Sarma, Phys. Rev. Lett. **105**, 077001 (2010).

[30] J. M. Maldacena, Adv. Theor. Math. Phys. **2**, 231 (1998).

[31] N. Beisert, C. Ahn, L. F. Alday, Z. Bajnok, J. M. Drummond *et al.*, Lett. Math. Phys. **99**, 1 (2012).

[32] Y. Jiang, S. Komatsu, and E. Vescovi, J. High Energy Phys. 07 (2020) 001.

[33] K. Hattori, Y. Hidaka, N. Yamamoto, and D.-L. Yang, J. High Energy Phys. 02 (2021) 001.

[34] D. Berenstein and S. Vazquez, J. High Energy Phys. 06 (2005) 059.

[35] Y. Qiao, J. Cao, W.-L. Yang, K. Shi, and Y. Wang, Phys. Rev. B **103**, L220401 (2021).

[36] X. Le, Y. Qiao, J. Cao, W.-L. Yang, K. Shi, and Y. Wang, J. High Energy Phys. 11 (2021) 044.

[37] W. Wang, Y. Qiao, J. Cao, W. M. Liu, and R. H. Liu, Nucl. Phys. **B975**, 115663 (2022).